Charge pumping in quantum wires

2004 J. Phys.: Condens. Matter 16 1789

(http://iopscience.iop.org/0953-8984/16/10/011)

INSTITUTE OF PHYSICS PUBLISHING JOURNAL OF PHYSICS: CONDENSED MATTER

J. Phys.: Condens. Matter **16** (2004) 1789–1802 PII: S0953-8984(04)66584-2

Charge pumping in quantum wires

E Faizabadi and F Ebrahimi

Department of Physics, Shahid Beheshti University, Tehran, Evin, 19839, Iran

E-mail: E-Faizabadi@cc.sbu.ac.ir and Ebrahimi@cc.sbu.ac.ir

Received 21 July 2003, in final form 27 November 2003
Published 27 February 2004
Online at stacks.iop.org/JPhysCM/16/1789 (DOI: 10.1088/0953-8984/16/10/011)

Abstract
The theory of charge pumping through a quantum wire is considered in the tight binding approximation. By introducing the Ricatti operator in the Hilbert space of the side-band states (Floquet states) we drive the Ricatti equation for a quantum wire driven by a time-periodic potential. Then a recursive method is developed for numerical calculation of the Floquet scattering matrix by expressing the right and left transmission and reflection operators in terms of the Ricatti operator. We then apply the method to the problem of charge pumping in a quantum wire attached to leads where the time-periodic potential (harmonic, pulsed and triangular) is applied to two sites of the wire. Finally, we show that the pumped current as a function of the wire–lead coupling shows a sign reversal.

1. Introduction

The subject of parametric electron pumping has attracted considerable attention in recent years [1–16]. An electron pump is a device which drives an electronic current by cyclic deformation of two or more system parameters [9, 10]. This interesting device operates at zero bias potential. The idea of producing current by cyclic deformation of the system parameters was originally proposed by Thouless [11]. Quite recently, this phenomenon was observed experimentally by Switkes *et al* [12] for an open quantum dot where the pumping signal was adiabatically produced by cyclic variation of the confining potential. They also observed that in the weak pumping regime the pumped current is sinusoidal in the phase difference of the deforming potential and non-sinusoidal in the strong pumping regime.

The original parametric pumping theory was formulated for the adiabatic regime [2, 10], which is valid up to first order in the pumping frequency. On the basis of the adiabatic theory [9, 10, 13], the total charge pumped per cycle is proportional to the area enclosed by the path in the parameter space, and non-zero current requires at least two parameters. This condition is met for the input potentials having non-zero phase difference. But, this theory is not consistent with the observed experimental results for zero phase difference [12]. The general expression for the averaged pumped current based on the time dependent S-matrix method for the adiabatic regime was derived by Brouwer [10]. It is important to note that the adiabatic condition dose not imply that the pumping amplitude should be small; in fact, the adiabatic condition requires the oscillation period of the system parameters to be much larger than the Wigner delay time, the time that characterizes the duration of the interaction. In an attempt to go beyond the adiabatic approximation, Zhu and Wang [14] have, on the basis of the Floquet theorem, developed a method for calculating the current in quantum pumps valid for all regimes. They calculated the pumped current through a mesoscopic region in the presence of a time-periodic potential. Interestingly, their method shows non-zero pumping current at zero phase difference for asymmetric pumping amplitudes, consistent with the observed experimental values [12]. In another attempt to go beyond the adiabatic approximation Wang *et al* [13] have developed a first-principles formulation for quantum pumps, using Keldysh non-equilibrium Green function theory. Their method also predicts non-zero current for zero phase difference. Recently, Moskalets and Büttiker [15] have developed a Floquet scattering theory for quantum mechanical pumps applicable to all regimes. For mesoscopic samples they predicted a sign reversal of the pumped current when the pump frequency is equal to the level spacing of the discrete states formed by the pumping potential. Kim [16] using the same approach determined the validity of the adiabatic theory by using the Wigner delay time, obtained from the Floquet scattering matrix. He also showed that the pumped current as a function of the potential asymmetry at zero phase difference shows a sign reversal.

In this paper we develop a recursive method for calculating the elements of the Floquet scattering matrix for a quantum wire driven by a time-periodic potential. Describing the quantum wire in the tight binding approximation we first define the Ricatti operator in the Hilbert space of the side-band states. We then derive the associated Ricatti equation. The recursive method is then obtained by expressing the right and left transmission and reflection operators in terms of the Ricatti operator. Next, we use the recursive method for determining the pumped currents for harmonic, time-periodic pulsed and triangular potentials as a function of the phase difference and the amplitude of the pumping potential. We then consider the variation of the pumped current for different frequencies as a function of the wire–lead coupling. We observe a sign reversal for the pumped current. We finally compare the observed sign reversal with the sign reversals predicted in [15, 16] and discuss an application of this effect.

The paper is organized as follows. In section 2, we present the general formulation of the parametric pumping for quantum wires in the tight binding approximation. In section 3, defining the Ricatti operator on the Hilbert space of the side-band states, we derive the Ricatti equation for a quantum wire driven by a time-periodic potential. We then show how the transmission and reflection operators can be expressed in terms of the Ricatti operator, which in conjunction with the Ricatti equation constitutes a recursive method for determining the elements of Floquet scattering matrix. In section 4.1, we calculate the pumped current for a harmonic pumping potential as a function of the phase difference, the amplitude of pumping potential and the wire–lead coupling strength. We show that the sign of the pumped current is dependent on the coupling strength and is zero for specific values of the coupling. In section 4.2, we present some applications of the results obtained in the previous sections. Finally, we end the paper with a conclusion.

2. General formula

In this section we consider a quantum wire in the tight binding approximation with a time dependent periodic potential

$$V(n,t) = \sum_{\mathrm{l}=\mathrm{r}'}^{\mathrm{r}} \delta_{\mathrm{l},n}[V_{\mathrm{l}} + 2\tilde{V}_{\mathrm{l}}\cos(\omega t + \phi_{\mathrm{l}})], \qquad (1)$$

with period $\tau = 2\pi/\omega$. The sum is over the sites where the potential acts. The time dependent Schrödinger equation in the tight binding approximation for an electron moving in the above potential has the form

$$\mathrm{i}\hbar\frac{\partial\phi(n,t)}{\partial t} = -t_{n,n+1}\phi(n+1,t) - t_{n,n-1}\phi(n-1,t) + V(n,t)\phi(n,t), \tag{2}$$

where $\hbar$ is Planck's constant, n labels the sites of the wire and $t_{n,n+1}$ is the hopping parameter for sites n and $n+1$. Equation (2) can be simplified by using the Floquet theorem. According to the Floquet theorem the wavefunction can be written as

$$\phi(n,t) = \mathrm{e}^{-\mathrm{i}E_{\mathrm{Fl}}t/\hbar}\psi(n,t), \tag{3}$$

where E_{Fl} is the Floquet energy and $\psi(n,t)$ is a periodic function with period $\tau = 2\pi/\omega$, which can be written as

$$\psi(n,t) = \sum_{m'=-\infty}^{\infty}\sqrt{\frac{2\pi}{\omega}}\mathrm{e}^{-\mathrm{i}m'\omega t}\psi_{m'}(n). \tag{4}$$

Using equations (3) and (4) in (2) and using the orthogonality of the side-band basis functions, $\{\sqrt{\omega/2\pi}\exp(-\mathrm{i}m\omega t)\}$, we have

$$\begin{aligned}(E_{\mathrm{Fl}} + m\hbar\omega)\psi_m(n) &= -t_{n,n+1}\psi_m(n+1) - t_{n,n-1}\psi_m(n-1)\\ &\quad + \sum_{\mathrm{l}=\mathrm{r}'}^{\mathrm{r}}\delta_{\mathrm{l},n}([V_{\mathrm{l}}\psi_m(n) + \tilde{V}_{\mathrm{l}}[\mathrm{e}^{\mathrm{i}\phi_{\mathrm{l}}}\psi_{m+1}(n) + \mathrm{e}^{-\mathrm{i}\phi_{\mathrm{l}}}\psi_{m-1}(n)]).\end{aligned} \tag{5}$$

To derive the Ricatti equation, we rewrite equation (5) in an operator form in the Hilbert space of the side-band states $\{|m\rangle\}$, $m = 0, \pm1, \pm2, \ldots$. The side-band states are defined such that

$$\langle t|m\rangle = \sqrt{\frac{\omega}{2\pi}}\mathrm{e}^{-\mathrm{i}m\omega t}, \qquad m = 0, \pm1, \pm2, \ldots. \tag{6}$$

Next, we define the operators $\hat{H}_0(\omega)$, $\hat{T}_+$ and $\hat{T}_-$ as follows:

$$\hat{H}_0(\omega)|m\rangle = m\hbar\omega|m\rangle, \qquad m = 0, \pm1, \pm2, \ldots, \tag{7}$$

$$\hat{T}_+|m\rangle = |m+1\rangle \tag{8}$$

and

$$\hat{T}_-|m\rangle = |m-1\rangle. \tag{9}$$

It is a simple matter to show that the above operators satisfy the following commutation relations:

$$[\hat{T}_+, \hat{T}_-] = 0, \tag{10}$$

$$[\hat{H}_0(\omega), \hat{T}_+] = \hbar\omega\hat{T}_+ \tag{11}$$

and

$$[\hat{H}_0(\omega), \hat{T}_-] = -\hbar\omega\hat{T}_-. \tag{12}$$

Furthermore, we have

$$\langle t|\hat{T}_+|m\rangle = \sqrt{\frac{\omega}{2\pi}}\mathrm{e}^{-\mathrm{i}(m+1)\omega t} \tag{13}$$

and

$$\langle t|\hat{T}_-|m\rangle = \sqrt{\frac{\omega}{2\pi}}\mathrm{e}^{-\mathrm{i}(m-1)\omega t}. \tag{14}$$

In terms of the side-band states $\{|m\rangle\}$, we can rewrite equation (4) as

$$|\psi(n)\rangle = \sum_{m'=-\infty}^{\infty} \psi_{m'}(n)|m'\rangle. \tag{15}$$

Also, we have

$$2\cos(\omega t + \phi_{\mathrm{l}})\psi_n(t) = \mathrm{e}^{\mathrm{i}\phi_{\mathrm{l}}}\langle t|\hat{T}_-|\psi(n)\rangle + \mathrm{e}^{-\mathrm{i}\phi_{\mathrm{l}}}\langle t|\hat{T}_+|\psi(n)\rangle. \tag{16}$$

Thus, equation (5) can be written as

$$[E_{\mathrm{Fl}} + \hat{H}_0(\omega)]|\psi(n)\rangle = -t_{n,n+1}|\psi(n+1)\rangle - t_{n,n-1}|\psi(n-1)\rangle + \hat{V}(n)|\psi(n)\rangle, \tag{17}$$

where $\hat{V}(n)$ is the potential operator, given by

$$\hat{V}(n) = \sum_{\mathrm{l}=\mathrm{r}'}^{\mathrm{r}} \delta_{\mathrm{l},n}[V_{\mathrm{l}} + \tilde{V}_{\mathrm{l}}(\mathrm{e}^{\mathrm{i}\phi_{\mathrm{l}}}\hat{T}_- + \mathrm{e}^{-\mathrm{i}\phi_{\mathrm{l}}}\hat{T}_+)]. \tag{18}$$

Equation (17) is our starting point for the derivation of the Ricatti equation. It has the formal form of the tight binding Schrödinger equation with $\hat{H}_0(\omega)$ and $\hat{V}(n)$ being operators acting on the Hilbert space of the side-band states. Equation (17) can be generalized for any time-periodic pumping potential given by the Fourier series

$$V(t) = \sum_{n=-\infty}^{\infty} a_n \mathrm{e}^{-\mathrm{i}n\omega t}. \tag{19}$$

The action of $V(t)$ on the side-band states has the form

$$V(t)|m\rangle = \left[a_0 + \sum_{n=1}^{\infty}(a_{-n}\mathrm{e}^{\mathrm{i}n\omega t} + a_n\mathrm{e}^{-\mathrm{i}n\omega t})\right]|m\rangle, \tag{20}$$

which, upon using equations (13) and (14), can be written as

$$V(t)|m\rangle = \left[a_0 + \sum_{n=1}^{\infty}(a_{-n}\hat{T}_-^n + a_n\hat{T}_+^n)\right]|m\rangle, \tag{21}$$

or

$$V(t)|m\rangle = \hat{V}(\hat{T}_-, \hat{T}_+)|m\rangle, \tag{22}$$

where

$$\hat{V}(\hat{T}_-, \hat{T}_+) = a_0\hat{I} + \sum_{n=1}^{\infty}(a_{-n}\hat{T}_-^n + a_n\hat{T}_+^n) \tag{23}$$

is the operator form of the time-periodic pumping potential.

3. Transmission and reflection operators

For definiteness and ease of presentation of the formulation, we consider the configuration of the quantum wire depicted in figure 1. The pumping potentials are applied to the wire at sites -1 and $+1$. Also, different hopping parameters between the sites where the potential is applied are chosen. With this choice, we can also consider the effect of the wire–lead coupling on the pumped current.

The solutions of equation (17) in regions $j \geqslant 2$ and $j \leqslant -2$ for the case where the incoming wave is in the nth channel and is incident from the left have the form [14]

$$|\psi(j)\rangle = \begin{cases} \mathrm{e}^{\mathrm{i}(j+2)k_n}|n\rangle + \displaystyle\sum_{m=-\infty}^{\infty}|m\rangle\mathrm{e}^{-\mathrm{i}(j+2)k_m}R_{mn}^{\mathrm{l}}, & j \leqslant -2, \\ \displaystyle\sum_{m=-\infty}^{\infty}|m\rangle\mathrm{e}^{\mathrm{i}(j-2)k_m}T_{mn}^{\mathrm{l}}, & j \geqslant 2, \end{cases} \tag{24}$$

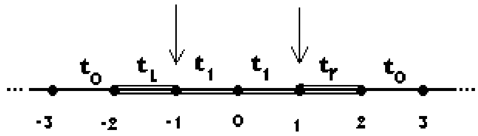

Figure 1. A schematic plot of a quantum wire.

where

$$R^{\mathrm{l}}_{mn} = \langle m|\hat{R}^{\mathrm{l}}|n\rangle \tag{25}$$

and

$$T^{\mathrm{l}}_{mn} = \langle m|\hat{T}^{\mathrm{l}}|n\rangle \tag{26}$$

are, respectively, the reflection and transmission amplitudes from the nth to the mth channel and k_n is the wavevector of the nth channel defined by $E_n = -2t_0\cos(k_n) + n\hbar\omega_0$. Defining a wavevector operator $\hat{k}$ such that

$$\hat{k}|m\rangle = k_m|m\rangle \qquad m = 0, \pm 1, \pm 2, \ldots, \tag{27}$$

and, using equations (25) and (26), we can rewrite the solution given by equation (24) in the form

$$|\psi(j)\rangle = \begin{cases} (\mathrm{e}^{\mathrm{i}(j+2)\hat{k}} + \mathrm{e}^{-\mathrm{i}(j+2)\hat{k}}\hat{R}^{\mathrm{l}})|n\rangle, & j \leqslant -2, \\ \mathrm{e}^{\mathrm{i}(j-2)\hat{k}}\hat{T}^{\mathrm{l}}|n\rangle, & j \geqslant 2. \end{cases} \tag{28}$$

On the basis of equation (28), we can define a new operator $\hat{\psi}(j)$, such that

$$|\psi(j)\rangle = \hat{\psi}(j)|n\rangle \qquad n = 0, \pm 1, \pm 2, \ldots. \tag{29}$$

For regions $j \leqslant -2$ and $j \geqslant 2$ this operator has the form

$$\hat{\psi}(j) = \begin{cases} \mathrm{e}^{\mathrm{i}(j+2)\hat{k}} + \mathrm{e}^{-\mathrm{i}(j+2)\hat{k}}\hat{R}^{\mathrm{l}}, & j \leqslant -2, \\ \mathrm{e}^{\mathrm{i}(j-2)\hat{k}}\hat{T}^{\mathrm{l}}, & j \geqslant 2. \end{cases} \tag{30}$$

Substituting equation (29) into the Schrödinger equation, we obtain the following equation for the operator $\hat{\psi}(j)$:

$$\hat{E}\hat{\psi}(j) = -t_{j,j+1}\hat{\psi}(j+1) - t_{j,j-1}\hat{\psi}(j-1) + \hat{V}(j)\hat{\psi}(j), \tag{31}$$

where

$$\hat{E} = E_{\mathrm{Fl}} + \hat{H}_0(\omega). \tag{32}$$

We now cast equation (31) into the Ricatti equation form by defining the Ricatti operator $\hat{Y}(j)$ by the relation

$$\hat{\psi}(j+1) = \hat{Y}(j)\hat{\psi}(j). \tag{33}$$

This operator satisfies the Ricatti equation [17]

$$\hat{Y}(j) = \frac{1}{t_{j,j+1}}[\hat{V}(j) - \hat{E}] - \frac{t_{j,j-1}}{t_{j,j+1}}\hat{Y}^{-1}(j-1). \tag{34}$$

The Ricatti equation can be used to obtain the left and right transmission operators, $\hat{T}^{\mathrm{l}}$ and $\hat{T}^{\mathrm{r}}$. Using equation (33), we have

$$\hat{\psi}(2) = \hat{Y}(1)\hat{\psi}(1), \tag{35}$$

but from equation (30) the left transmission operator is given by

$$\hat{\psi}(2) = \hat{T}^{\mathrm{l}}; \tag{36}$$

thus

$$\hat{T}^{\mathrm{l}} = \hat{Y}(1)\hat{\psi}(1). \tag{37}$$

Also, we have

$$\hat{\psi}(-2) = \hat{I} + \hat{R}^{\mathrm{l}}. \tag{38}$$

Upon using equation (33) in (37), we obtain for the left transmission operator

$$\hat{T}^{\mathrm{l}} = \hat{Y}(1)\hat{Y}(0)\hat{Y}(-1)\hat{Y}(-2)\hat{\psi}(-2), \tag{39}$$

or

$$\hat{T}^{\mathrm{l}} = \hat{Y}(1)\hat{Y}(0)\hat{Y}(-1)\hat{Y}(-2)(\hat{I} + \hat{R}^{\mathrm{l}}), \tag{40}$$

where according to equation (38) and the Ricatti equation the left reflection operator is given by

$$\hat{R}^{\mathrm{l}} = \{[\hat{Y}^{-1}(-3) - \mathrm{e}^{\mathrm{i}\hat{k}}]^{-1}[-2\mathrm{i}\sin\hat{k}]\} - \hat{I}. \tag{41}$$

Also, we have

$$\hat{\psi}(3) = \hat{Y}(2)\hat{\psi}(2), \tag{42}$$

which gives us the initial data

$$\hat{Y}(2) = \mathrm{e}^{\mathrm{i}\hat{k}}. \tag{43}$$

The same procedure can be applied for the case where the incoming wave is incident from the right. The transmission and reflection operators in this case are

$$\hat{T}^{\mathrm{r}} = \hat{Y}^{-1}(-2)\hat{Y}^{-1}(-1)\hat{Y}^{-1}(0)\hat{Y}^{-1}(1)(\hat{I} + \hat{R}^{\mathrm{r}}) \tag{44}$$

and

$$\hat{R}^{\mathrm{r}} = \{[\hat{Y}(2) - \mathrm{e}^{-\mathrm{i}\hat{k}}][2\mathrm{i}\sin\hat{k}]\} - \hat{I}, \tag{45}$$

with initial data

$$\hat{Y}(-3) = \mathrm{e}^{\mathrm{i}\hat{k}}. \tag{46}$$

Finally, we determine the left and right transmission and reflection operators for the case where the input pumping potential acts at the general sites $-m$ and n. Following the steps described in this section, we obtain the following expressions for the left and right transmission and reflection operators:

$$\hat{T}^{\mathrm{l}} = \hat{Y}(n)\hat{Y}(n-1)\cdots\hat{Y}(0)\hat{Y}(-1)\hat{Y}(-2)\cdots\hat{Y}(-m-1)(\hat{I} + \hat{R}^{\mathrm{l}}), \tag{47}$$

$$\hat{R}^{\mathrm{l}} = \{[\hat{Y}^{-1}(-m-2) - \mathrm{e}^{\mathrm{i}\hat{k}}]^{-1}[-2\mathrm{i}\sin\hat{k}]\} - \hat{I}, \tag{48}$$

$$\hat{T}^{\mathrm{r}} = \hat{Y}^{-1}(-m-1)\hat{Y}^{-1}(-m)\cdots\hat{Y}^{-1}(0)\hat{Y}^{-1}(1)\cdots\hat{Y}^{-1}(n)(\hat{I} + \hat{R}^{\mathrm{r}}) \tag{49}$$

and

$$\hat{R}^{\mathrm{r}} = \{[\hat{Y}(n+1) - \mathrm{e}^{-\mathrm{i}\hat{k}}][2\mathrm{i}\sin\hat{k}]\} - \hat{I}, \tag{50}$$

with initial data equal to $\mathrm{e}^{\mathrm{i}\hat{k}}$, at sites $n + 1$ and $-m - 2$. Equations (47)– (50) in conjunction with equation (34) provide a recursive method for numerical calculation of the elements of the Floquet scattering matrix

$$\hat{S} = \begin{pmatrix} \hat{R}^{\mathrm{l}} & \hat{T}^{\mathrm{r}} \\ \hat{T}^{\mathrm{l}} & \hat{R}^{\mathrm{r}} \end{pmatrix}. \tag{51}$$

Depending on the chosen dimension of the side-band space, the matrix equations for the Ricatti operator with the initial conditions can be solved numerically, and these in turn can be used for numerical calculation of the transmission and reflection operators.

4. Results

In section 4.1 we apply the method developed in the previous section to calculate the pumped current at zero temperature as a function of the phase difference, the amplitude of pumping potential and the wire–lead coupling strength for harmonic input pumping potential, applied to sites −1 and +1. In section 4.2, we consider the applications of the formalism developed in the previous section. For all the calculations the dimensions of the side-band space are taken to be equal to 41. This gives an accuracy of better than 10^{-8} for the calculated pumped currents.

4.1. Harmonic pumping potential

For the input harmonic pumping potential the potential operator in the Ricatti equation is everywhere zero except at sites −1 and +1; it is given by

$$\hat{V}(-1) = V_-(\hat{T}_- + \hat{T}_+) \tag{52}$$

and

$$\hat{V}(+1) = V_+(\hat{T}_- \mathrm{e}^{\mathrm{i}\phi} + \hat{T}_+ \mathrm{e}^{-\mathrm{i}\phi}), \tag{53}$$

where ϕ is the phase difference. If the system is in contact with ideal leads with identical chemical potentials μ, the averaged pumped current per period, $\tau = 2\pi/\omega_0$, is given by

$$I(\mu) = \frac{e}{\pi\hbar} \int_{-2t_0}^{2t_0} \mathrm{d}E\, g(E) f(E-\mu) T_{\mathrm{net}}(E) \tag{54}$$

where $g(E)$ is the density of states of the wire, $f(E)$ is the Fermi–Dirac distribution function at zero temperature and $T_{\mathrm{net}}(E)$ is the net transmission coefficient divided by the density of states. This latter term for the incoming wave in the side-band state $n = 0$ with energy E is given by the equation

$$T_{\mathrm{net}}(E) = \frac{1}{g(E)} \sum_{m=0}^{\infty} \left| \frac{\sin(k_m)}{\sin(k_0)} \right| [|T^{\mathrm{r}}_{m,0}(E)|^2 - |T^{\mathrm{l}}_{m,0}(E)|^2]. \tag{55}$$

In the above equation $T^{\mathrm{r}}_{n,m}$ and $T^{\mathrm{l}}_{n,m}$ are, respectively, matrix elements of the transmission operators in the space of side-band states, which according to equations (40), (41), (44) and (45) can be written as

$$T^{\mathrm{l}}_{n,m} = \langle n|\hat{Y}(1)\hat{Y}(0)\hat{Y}(-1)\hat{Y}(-2)\{[\hat{Y}^{-1}(-3) - \mathrm{e}^{\mathrm{i}\hat{k}}]^{-1}[-2\mathrm{i}\sin\hat{k}]\}|m\rangle \tag{56}$$

and

$$T^{\mathrm{r}}_{n,m} = \langle n|\hat{Y}^{-1}(-2)\hat{Y}^{-1}(-1)\hat{Y}^{-1}(0)\hat{Y}^{-1}(1)\{[\hat{Y}(2) - \mathrm{e}^{-\mathrm{i}\hat{k}}]^{-1}[2\mathrm{i}\sin\hat{k}]\}|m\rangle. \tag{57}$$

For chemical potential, μ, equal to zero and the hopping parameters, $t_{n,n+1}$, equal to one, the pumped current for the weak regime is calculated for $V_+ = V_-$ as a function of the phase difference. The results for three different frequencies are depicted in figure 2. We have the known sinusoidal behaviour of the adiabatic theory. Figure 3 represents the pumped currents for the same configurations but for the strong pumping regime. The pumped currents for the asymmetric cases, $V_+ \neq V_-$, as a function of the phase difference are depicted in figure 4. We have the same results as reported by Zhu and Wang [14]; for the zero phase difference the pumped currents are non-zero. Finally, by taking the values of t_{l} and t_{r} equal to each other, but different to the rest, we can consider the segments $n < -1$ and $n > 1$ as the left and right leads, respectively, and $t_{\mathrm{l}} = t_{\mathrm{r}} = t$ as the term for the coupling between the wire and leads. Figures 5(a) and (b) represent the pumped currents for the weak and strong regimes, respectively, as a function of t for the phase difference equal to $\pi/4$ and $\pi/2$. It can be seen

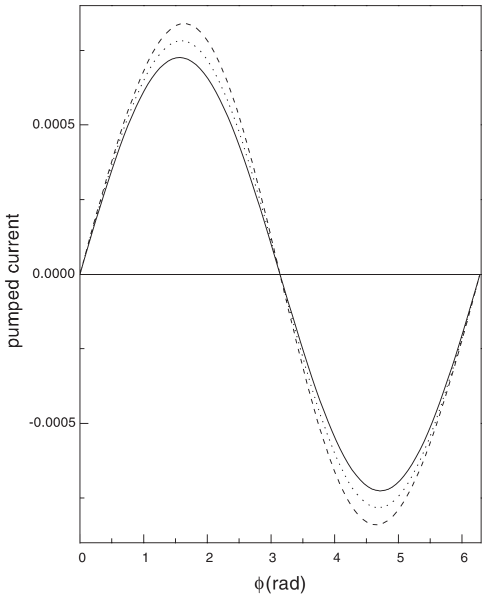

Figure 2. The pumped currents in units of $et_0/\pi\hbar$ for frequencies $\omega = 0.2$ (dashed curve), $\omega = 0.3$ (dotted curve) and $\omega = 0.4$ (solid curve) as a function of the phase difference ϕ, for harmonic input signals. The energy scale is t_0, $E_F = 0.0$, $t_l = t_r = t_1 = t_0 = 1.0$ and $V_+ = V_- = 0.1$ (weak regime).

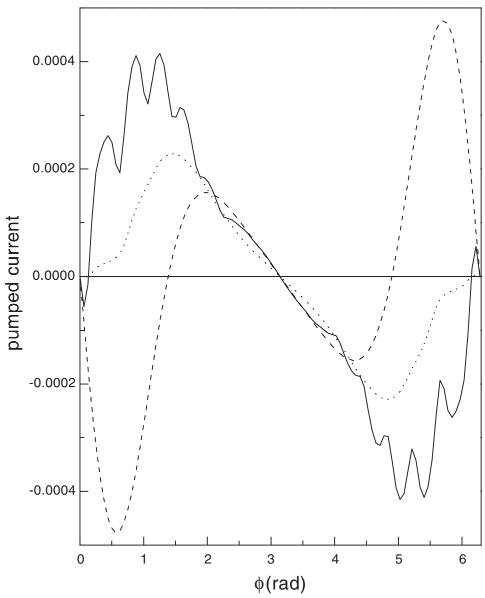

Figure 3. The pumped currents in units of $et_0/\pi\hbar$ for frequencies $\omega = 0.2$ (dashed curve), $\omega = 0.3$ (dotted curve) and $\omega = 0.4$ (solid curve) as a function of the phase difference ϕ, for harmonic input signals. The energy scale is t_0, $E_F = 0.0$, $t_l = t_r = t_1 = t_0 = 1.0$ and $V_+ = V_- = 0.6$ (strong regime).

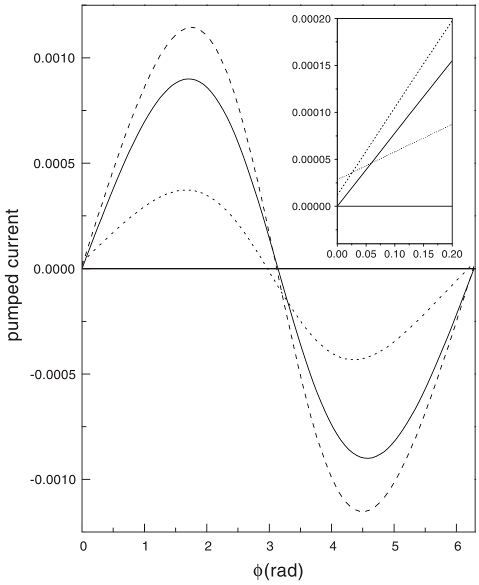

Figure 4. The pumped currents in units of $et_0/\pi\hbar$ for frequency $\omega = 0.1$ as a function of the phase difference ϕ, for input signal strengths $V_+ = 0.1$, $V_- = 0.2$ (dashed curve), $V_+ = 0.1$, $V_- = 0.4$ (dotted curve) and $V_+ = 0.1$, $V_- = 0.1$ (solid curve). The energy scale is t_0, $E_F = 0.0$ and $t_l = t_r = t_1 = t_0 = 1.0$.

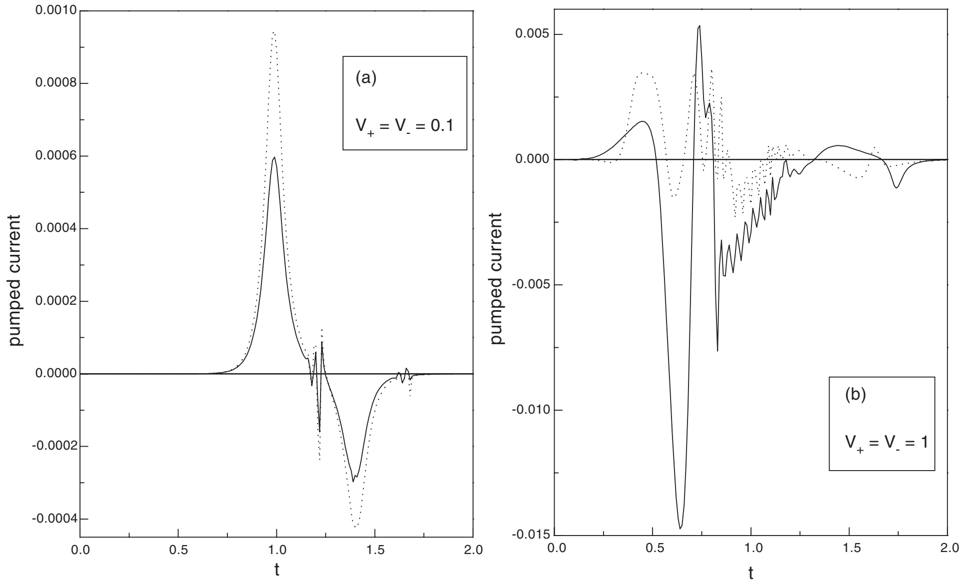

Figure 5. The pumped currents in units of $et_0/\pi\hbar$ for $\phi = \pi/2$ (dotted curve) and $\phi = \pi/4$ (solid curve) versus the parameter of the coupling between the wire and leads, (a) for weak regimes: the energy scale is t_0, $E_F = 0.0$, $\omega = 0.1$ and $t_1 = t_0 = 1.0$; (b) for strong regimes: the energy scale is t_0, $E_F = 0.0$, $\omega = 0.4$ and $t_1 = t_0 = 1.0$.

that the sign of the pumped current depends on the strength of the coupling between the wire and leads and a sign reversal can occur by varying the t. We now discuss the origin of this sign reversal. For simplicity, the coupling of the wire to the left and right leads for $t > 1$ is considered as a static double barrier and for $t < 1$ as a static double well. The double barrier (double well) creates resonance states within the energy band of the quantum wire. The effect of a time-periodic pumping potential on the incoming waves with energy E is to scatter them to different Floquet states with energy $E + m\hbar\omega_0$, where $m = 0, \pm 1, \pm 2, \ldots$. Therefore, the reflected and transmitted waves are superpositions of the Floquet states. But each of the Floquet states due to the scattering from the static double barrier (double well) acquires an extra phase shift. Since the scattering phase shift is an energy dependent quantity, each Floquet state acquires a different phase shift. Thus, an extra phase difference between any two Floquet states appears, which depends on the height of the double barrier (the depth of the double well), i.e. on the strength of the wire–lead coupling. Thus the wire–lead coupling contributes an additional term to the total phase difference. Since the pumped current is an odd function of the phase difference, whenever this additional phase difference becomes equal to odd multiples of π the pumped current changes sign. The additional phase difference can also cause sign reversal as a function of frequency. This can happen whenever absorption (emission) of energy from the input pumping potential causes the incoming wave with energy below (above) the energy of a resonance state to make a transition to a Floquet state with energy above (below) the energy of a resonance state.

4.2. Applications

In this section we consider some applications of the results obtained in the previous sections. We first consider the application of the recursive method to the general time-periodic potential. Then we discuss an application of the sign reversal.

The representation of the left and right transmission operators in terms of the Ricatti operator and the general expression of the input pumping potential in terms of $\hat{T}_+$ and $\hat{T}_-$ operators, equation (23), provide a simple and fast way for numerically calculating the pumped current for an arbitrary time-periodic input potential.

We first determine the pumped current for a time-periodic pulsed input potential acting at sites -1 and $+1$. The potential operator is zero everywhere except at the aforementioned sites; it is given by

$$\hat{V}(-1) = V_- \left\{ a_0 \hat{I} + \sum_{n=1}^{\infty} [a_{-n} \mathrm{e}^{\mathrm{i}n\phi} \hat{T}_-^n + a_n \mathrm{e}^{-\mathrm{i}n\phi} \hat{T}_+^n] \right\} \tag{58}$$

and

$$\hat{V}(+1) = V_+ \left\{ a_0 \hat{I} + \sum_{n=1}^{\infty} [a_{-n} \hat{T}_-^n + a_n \hat{T}_+^n] \right\}, \tag{59}$$

where

$$a_0 = \frac{\tau'}{\beta} \tag{60}$$

and

$$a_n = \frac{2}{n\omega\beta} \sin\left(\frac{n\omega\beta}{\tau'}\right) \qquad n = \pm 1, \pm 2, \ldots, \tag{61}$$

which τ' is the duration of the pulse, β its period, and V_- and V_+ are the amplitudes. The calculated pumped current as a function of the phase difference, $\Delta\phi = \phi$, for the weak pumping regime is presented in figure 6. We have also carried out the calculation for the triangular shape time-periodic input potential for which the potential operators at sites -1 and $+1$ are given by

$$\hat{V}(-1) = V_- \left\{ a_0 \hat{I} + \sum_{n=1}^{\infty} [a_{-n} \mathrm{e}^{\mathrm{i}n\phi} \hat{T}_-^n + a_n \mathrm{e}^{-\mathrm{i}n\phi} \hat{T}_+^n] \right\} \tag{62}$$

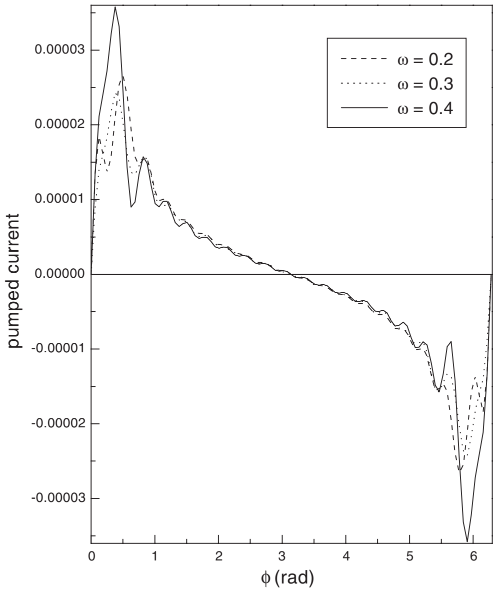

Figure 6. The pumped currents in units of $et_0/\pi\hbar$ versus the phase difference ϕ, for pulsed periodic potential. The energy scale is t_0, $E_F = 0.0$, $t_l = t_r = t_1 = t_0 = 1.0$, $V_+ = V_- = 0.1$ and $\tau' = 2\pi$.

and

$$\hat{V}(+1) = V_+\left\{a_0\hat{I} + \sum_{n=1}^{\infty}[a_{-n}\hat{T}_-^n + a_n\hat{T}_+^n]\right\}, \tag{63}$$

where

$$a_0 = 0 \tag{64}$$

and

$$a_n = \frac{4}{n^2\pi^2} \qquad n = \pm1, \pm2, \ldots. \tag{65}$$

The results are depicted in figure 7.

Finally, we discuss an application of the sign reversal. Figure 8 represents the plots of frequency versus the smallest value of the strength of the coupling between the wire and leads where the current becomes zero. The graphs correspond to three different amplitudes for the pumping potential. The pumped current becomes zero wherever the total phase difference becomes equal to zero or integer multiples of π. For the configuration we have chosen for the quantum pump, the total phase difference, $\Delta\phi$, is a sum of three terms, $\Delta\phi_1$, $\Delta\phi_2$ and $\Delta\phi_3$; i.e. $\Delta\phi = \Delta\phi_1 + \Delta\phi_2 + \Delta\phi_3$. The first term, $\Delta\phi_1$, is the phase difference of the pumping potential. For the results depicted in figure 8 this is fixed at $\pi/2$. The second term is the phase difference predicted in [15]. This phase difference is a manifestation of the existence of two different amplitudes for the absorption (emission) of energy from the pumping potential. Since these two amplitudes are spatially separated, a phase difference between them appears. In the adiabatic regime for an oscillating double barrier with separation l (the model used in [15]) this phase difference is proportional to $(\sqrt{E} - \sqrt{E + \hbar\omega})l$, where the energy E is close to the Fermi energy of the leads. It is independent of the strength of the wire–lead coupling. The third term is the phase difference caused by the scattering of the Floquet states from the static

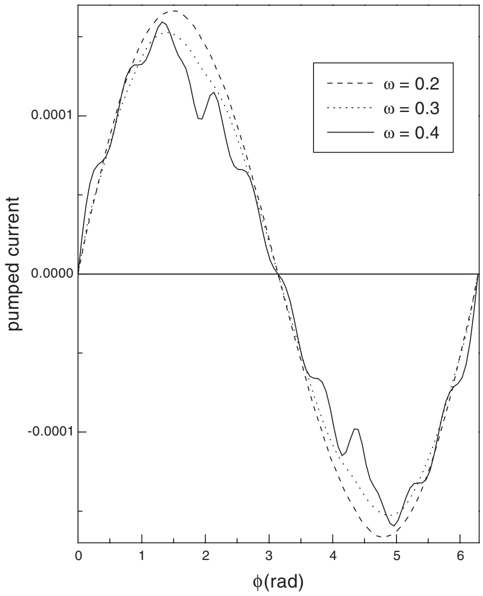

Figure 7. The pumped currents in units of $et_0/\pi\hbar$ versus the phase difference ϕ, for a periodic triangular potential. The energy scale is t_0, $E_F = 0.0$, $t_l = t_r = t_1 = t_0 = 1.0$ and $V_+ = V_- = 0.1$.

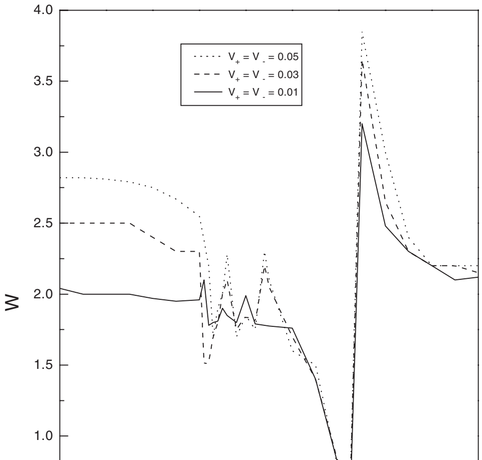

Figure 8. Plots of the frequency versus the smallest value of the strength of the coupling between the wire and leads where the pumped currents become zero. The energy scale is t_0, $E_F = 0.0$, $t_1 = t_0 = 1.0$ and $\phi = \pi/2$.

double barrier (double well), formed by the coupling between the wire and leads. This phase difference and its variation depend on the locations and the widths of the resonance states. For

t from 0.6 to 0.8 and from 1.4 to 1.6 the locations of zeros are approximately independent of t. In these ranges the behaviour of the total phase difference is dominated by $\Delta\phi_2$. For t between 0.8 and 1.4 the major contribution to the total phase difference is due to $\Delta\phi_3$. In this region resonance states appear below ($t < 1$) and above ($t > 1$) the Fermi energy. Within the range $0.9 < t < 1.1$, the resonance states are close to the Fermi energy with short lifetimes (wide width). The peak at $t = 1.22$ is mainly caused by a narrow resonance state, not too close to the Fermi energy. In principle, by searching for a frequency that makes the current equal to zero, plots like figure 8 can be used for the experimental determination of the strength of the coupling between the wire and leads.

5. Conclusion

To summarize, the Hilbert space of the side-band states is the most natural space in which to formulate the theory of quantum pumps. The recently proposed Floquet scattering matrix [15], for charge pumping in the mesoscopic conductors, is an operator in this space. Therefore, formulating the general theory of the quantum pump in this space might be of considerable importance. In this work, first, using the tight binding approximation, we showed how this can be done for a quantum wire driven by a time-periodic potential. Furthermore, by defining the Ricatti operator in this space, we have derived the Ricatti equation. This allowed us to express the right and left transmission and reflection operators (the elements of the Floquet scattering matrix) in terms of the Ricatti operator which in turn can be used for a recursive calculation of the Floquet scattering matrix. Next, we used the aforementioned recursive method for numerical calculation. We have calculated the pumped current as a function of the phase difference, the amplitude of the pumping potential and the strength of the wire–lead coupling. We have shown that the current as a function of the wire–lead coupling shows a sign reversal. In section 4.2, we discussed the origin of this sign reversal, which is different to the sign reversals predicted in [15, 16]. As discussed in section 4.2, the total phase difference is the sum of contributions from the phase difference of the pumping potential, the phase difference predicted in [15] and the phase difference caused by the scattering of the Floquet states from the double barrier (double well) formed by the coupling of the wire to the leads. Since the pumping potential that we have used is spatially symmetric, the results of [16] are not relevant to the sign reversal that we have observed. Finally, we have pointed out how, in principle, the zeros of the current as a function of the frequency and the wire–lead coupling can be used for the experimental determination of the strength of coupling between the wire and leads.

Acknowledgments

One of us, E Faizabadi, acknowledges the assistance of Dr A Koohi, Dr T Vazifehshenas and M Bagheri.

References

[1] Niu Q 1990 *Phys. Rev.* B **64** 1812
[2] Zhou F, Spivak B and Altshuler B L 1999 *Phys. Rev. Lett.* **82** 608
[3] Altshuler B L and Glazman L I 1999 *Science* **283** 1864
[4] Vavilov M *et al* 2001 *Phys. Rev.* B **63** 195313
[5] Levinson Y, Entin-Wohlman O and Wölfle P 2000 *Phys. Rev. Lett.* **85** 634
[6] Wagner M 2000 *Phys. Rev. Lett.* **85** 174
[7] Wei Y, Wang J and Guo H 2000 *Phys. Rev.* B **62** 9947
[8] Shutenko T A, Aleiner I L and Altshuler B L 2000 *Phys. Rev.* B **61** 10366

[9] Aleiner I L and Andreev A V 1998 *Phys. Rev. Lett.* **81** 1286
[10] Brouwer P W 1998 *Phys. Rev.* B **58** R10, 135
[11] Thouless D J 1983 *Phys. Rev.* B **27** 6083
[12] Switkes M, Marcus C and Capman K 1999 *Science* **283** 1905
[13] Wang B, Wang J and Guo H 2002 *Phys. Rev.* B **65** 073306
[14] Zhu S-L and Wang Z D 2002 *Phys. Rev.* B **65** 155313
[15] Moskalets M and Büttiker M 2002 *Phys. Rev.* B **66** 205320
[16] Kim S W 2002 *Phys. Rev.* B **66** 235304
[17] Heinrichs J 2001 *Preprint* cond-mat/0106432